AD_____
(Leave blank)

Award Number: W81XWH-08-1-0352

TITLE: Optimizing and Evaluating an Integrated SPECT-CmT System Dedicated to Improved 3-D Breast Cancer Imaging

PRINCIPAL INVESTIGATOR: Dominic Crotty

CONTRACTING ORGANIZATION: Duke University, Durham, NC, 27710

REPORT DATE: May 2010

TYPE OF REPORT: Annual Summary

PREPARED FOR: U.S. Army Medical Research and Materiel Command Fort Detrick, Maryland 21702-5012

DISTRIBUTION STATEMENT: (Check one)

x Approved for public release; distribution unlimited

Distribution limited to U.S. Government agencies only; report contains proprietary information

REPORT DOCUMENTATION PAGE

Form Approved
OMB No. 0704-0188

1. REPORT DATE *(DD-MM-YYYY)*	2. REPORT TYPE	3. DATES COVERED *(From - To)*
05-01-2010	Annual Summary~	01 MAY 2008-30 APR 2010

4. TITLE AND SUBTITLE
Optimizing and Evaluating an Integrated SPECT-CmT System Dedicated to Improved 3-D Breast Cancer Imaging

5a. CONTRACT NUMBER

5b. GRANT NUMBER
W81XWH-08-1-0352

5c. PROGRAM ELEMENT NUMBER

6. AUTHOR(S)
Dominic Crotty
Email: dominic.crotty@duke.edu

5d. PROJECT NUMBER

5e. TASK NUMBER

5f. WORK UNIT NUMBER

7. PERFORMING ORGANIZATION NAME(S) AND ADDRESS(ES)
Duke University
Durham, NC

8. PERFORMING ORGANIZATION REPORT NUMBER

9. SPONSORING / MONITORING AGENCY NAME(S) AND ADDRESS(ES)
US Army Medical Research and Material Command
Fort Detrick, Maryland
21702-5102

10. SPONSOR/MONITOR'S ACRONYM(S)

11. SPONSOR/MONITOR'S REPORT NUMBER(S)

12. DISTRIBUTION / AVAILABILITY STATEMENT
Approved for public release ; distribution unlimited

13. SUPPLEMENTARY NOTES

14. ABSTRACT
The overall objective of this research is to optimize the development of a combined dual-modality single photon emission computed tomography (SPECT) and x-ray computed mammotomography (CmT) system for the earlier detection and staging of breast cancer, improving surgical biopsy guidance, and the monitoring of patient therapy response. It is believed that co-registered acquisition of emission (nuclear) and transmission (x-ray) data using both 3D imaging modalities in a common field of view may aid to accurately localize the radioactive uptake of a tumor in the emission image by using anatomical structure from the transmission image. In this second year, the radiation dose absorbed by the uncompressed breast during a regular tomographic scan using is extensively quantified using the developed tomographic system. New concept designs for the next generation 3D breast CmT system are also developed, in addition to new tomographic trajectories designed to overcome limitations in the ability of the developed CmT system to view the chest wall of the prone patient. In addition to the technical work, other aspects of the training program were also completed, including site visits to a major medical imaging company, the presentation of the research at scientific conferences, and the ongoing submission of a manuscript to a major peer reviewed journal. Finally, the doctoral thesis arising from this research was written and successfully defended by the author.

15. SUBJECT TERMS
X-ray imaging, Nuclear Medicine Imaging, SPECT, CT, Molecular Breast Imaging, Mammotomography

16. SECURITY CLASSIFICATION OF:			17. LIMITATION OF ABSTRACT	18. NUMBER OF PAGES	19a. NAME OF RESPONSIBLE PERSON
a. REPORT	b. ABSTRACT	c. THIS PAGE			Dominic Crotty
Unclassified	Unclassified	Unclassified	Unlimited	31	19b. TELEPHONE NUMBER 919 544 6058

Table of Contents

A. INTRODUCTION

The objective of this project is to enhance the development of a combined dual-modality single photon emission computed tomography (SPECT) and x-ray computed mammotomography (CmT) system for the earlier detection and staging of breast cancer. Co-registered acquisition of emission (nuclear) and transmission (x-ray) data using both 3D imaging modalities in a common field of view may help to accurately localize the radioactive tumor uptake in the emission image by using the anatomical structure visible in the transmission image.

In the second year of this three year grant the dose absorbed by the uncompressed and pendant breast during a dedicated computed tomography breast scan was measured using radiochromic film, calibrated using thermoluminescent detectors and an ion chamber. The dose absorbed during a scan is initially measured using geometric phantoms of various shapes and filled with liquids that simulate different breast compositions. Ultimately, a breast cadaver is scanned using the regular tomographic protocol and the absorbed dose again measured using calibrated radiochromic film. This is a large step forward in the sense that this empirical method can now be used instead of the previous simulation based methods. In further work, a new design was developed for the next generation breast scanner device to enable fully 3D motion for the CT scanner. This design also incorporated a new bed design for prone patient imaging that would allow for increased coverage of the pendant breast volume.

In addition to this extensive set of experiments, several aspects of the training program were completed, including presentations at domestic and international conferences, a site visit to a major medical imaging company to discuss my research, submission of a manuscript for peer review, publishing of manuscripts in conference proceedings. Ultimately, the doctoral thesis arising from this research was successfully written and defended at the end of this grant year.

B. BODY

The Statement of Work along with the original projected timeline is attached in Appendix A of this Report. In Year 2, a modified Task 1 was completed that included aspects of the experiments that were not proposed in the original set of work but that added immensely to the overall quality of the work. Additionally, aspects of Task 3 were also completed. The system as it stands currently is shown in Figure 1. This system was updated since Year 1 of the project.

Task 1: Optimize tradeoffs between absorbed dose and image quality for the CmT subsystem

Task 1(a) Embed thermoluminescent dosimeters or available MOSFET detectors in anthropomorphic breast phantoms to evaluate dose for various sizes and compositions of breast equivalent tissue and lesions

The integrated SPECT-CmT system in its current form, described in detail in the report for Year 1 of this report, is shown in Figure 1[1-2].

Task 1 was completed using an initial set of phantom-based experiments that ultimately culminated in the scanning of a human breast cadaver to quantify the absorbed dose during a tomographic scan. This added an extra dimension to the study that was proposed in the Statement of Work. As proposed, embedded thermoluminescent detectors (TLDs) were used in the experiments but, after consultation with experts in the field of radiation dosimetry, it was decided to instead complete the experiments using a novel 2D dosimetry technique using radiochromic film (GafChromic™, *International Specialty Products,* Wayne, NJ)[3-5]. An interdepartmental collaboration was established with the Radiation Dosimetry facility at Duke University Medical Center, who provided expertise in the quantification of absorbed dose, and who also provided the

radiochromic film and TLDs. In their expert opinion, it was prohibitively expensive to use TLDs for the various study setups and that the dosimetry results from one setup could be extended to similar setups that simply used other current and voltage settings for the imaging prootocol.

The genesis of this study came from the fact that dedicated breast CT acquires many hundreds of individual 2D x-ray projection images that are subsequently reconstructed to generate the 3D volume of the breast. The cumulative dose absorbed by the breast during a tomographic scan is then of paramount importance to imaging system design. For dual-view x-ray mammography, guidelines from the American College of Radiology (ACR) require that the average absorbed dose to a 4.2cm-thick compressed breast consisting of 50-50% adipose-glandular tissue not exceed 6mGy[6]. Dedicated breast CT imaging, a technology still in its infancy, lacks an equivalent and established dose standard for uncompressed breast imaging. Therefore, as a starting point in system development and optimization, dedicated breast CT system designers aim to confine the cumulative absorbed dose for a complete breast CT scan to one that approximates dual view mammography; such was the case in this system development.

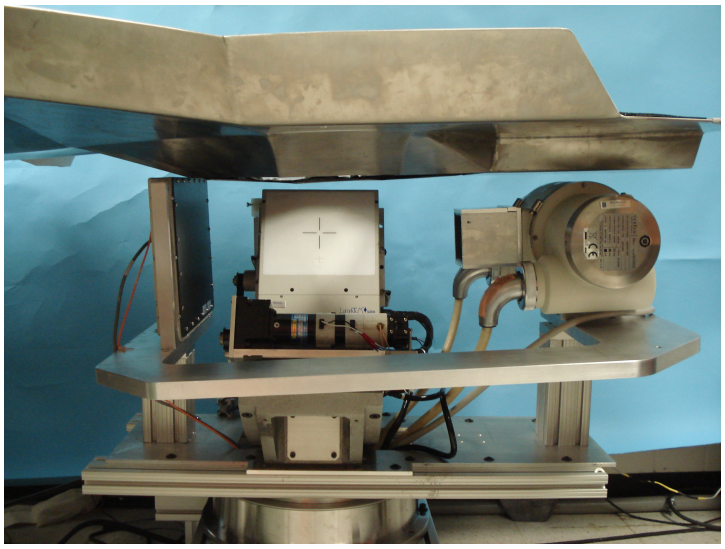

FIGURE 1 Image of the custom deisgned patient bed positioned over the prototype integrated SPECT-CmT imaging system.

Breast CT has generally been estimated using a combination of measurements in air, computer-modeling of x-ray tube spectra incident on the breast, and 3D Monte Carlo simulations. In contrast to previous simulation studies, this study empirically quantifies the dose imparted to a pendant uncompressed cadaveric breast, and illustrates the 2D spatial dose distribution obtained using our dedicated 3D breast CT imaging system[7-11].

Initially, TLDs and XRQA film were cross-calibrated with a 6cm^3 ionization chamber (Mammochamber, Model 10x5-6M-3, *RadCal*, Monrovia, CA). Separate sets of dosimeters including one piece of film, two TLDs, and the ion chamber were exposed in air to four separate exposure levels with the quasi-monochromatic x-ray beam of the dedicated breast CT, ranging from 659.5mR to 1.915R. Dosimeter calibration plots for the XRQA film were fit using least-squares regression techniques. In this case, the TLD and exposure meter measurements are considered the gold standard to which the radiochromic film is calibrated and evaluated.

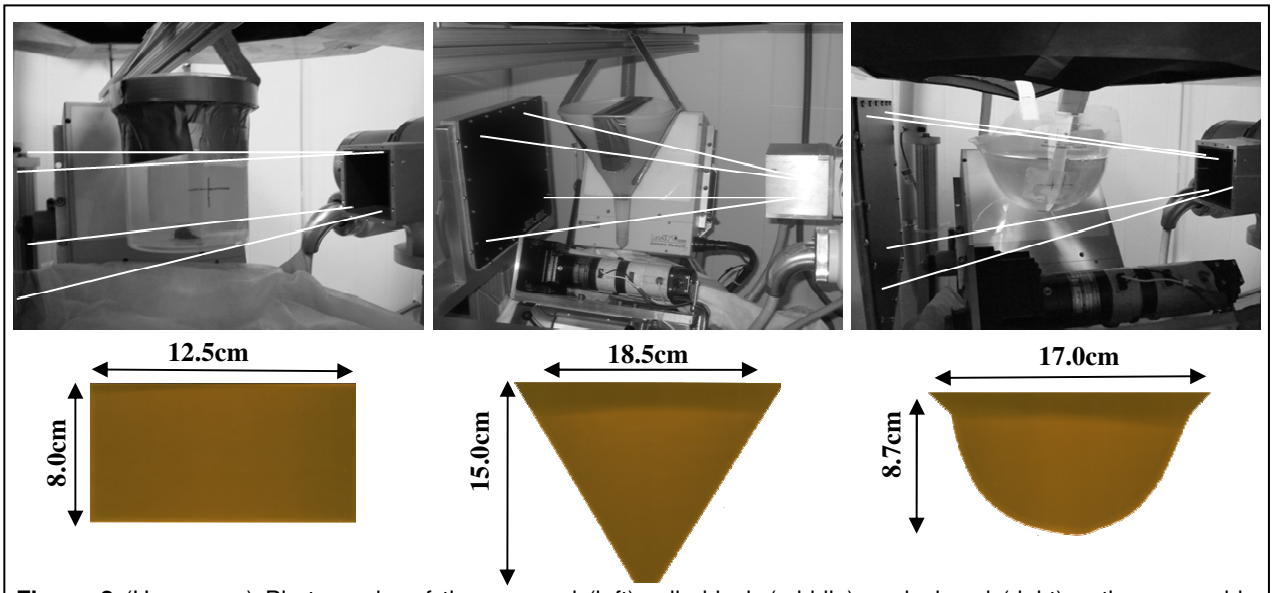

Figure 2 (Upper row) Photographs of the scanned (left) cylindrical, (middle) conical and (right) anthropomorphic breast phantoms, respectively. A representation of the approximate position of the x-ray cone beam emanating from the x-ray tube is superimposed over each setup. (Lower Row) Radiochromic films of the same cross-sectional shapes showing dimensions of the films for the tested phantoms.

Breast phantom volumes, shown in Figure 2, were initially filled with mineral oil and water to examine the variation in absorbed dose for what would be the expected boundary conditions of 100% fatty or 100% glandular breast tissue composition, respectively.

For both of these scatter media, three different breast phantom shapes were tested to observe variations in absorbed breast dose as a function of the shape and the effective radius of the breast phantoms. Two of the phantoms were in the shape of a cylinder and a cone, while the third was in the anthropomorphic shape of a breast. The regular cylindrical phantom presented a constant cross section of absorbing material to the divergent x-ray cone beam, simulating the setup often used in Monte Carlo dose studies. The conical shape phantom more closely resembled the shape of a pendant breast, decreasing in radius from chest wall to nipple, but it did so in a uniform fashion. From previous studies it was observed that approximately 15% of subjects have this conically shaped pendant breast. The anthropomorphic breast shape was then a natural progression from the prior geometric shapes and represented a 60% prevalent clinical geometric pendant breast shape, dimension and volume.

For each phantom, a single sheet of XRQA film, cut to match the cross-sectional template of the phantom, was attached to the inside surface of the phantom. The dimensions of the various cross-sectional templates are shown in Figure 2. The phantoms were positioned as close to the isocenter of the cone beam CT imaging system as possible (Figure 2), and scanned using the tomographic imaging protocol: 240 projections equally spaced over 360°.25mA and 100ms per projection, at a tube voltage of 60kVp. A simple circular scanning protocol, with the system rotating around a vertical axis, was employed. The phantoms were initially filled with 1000mL of water (ρ = 1.0 g/cm^3) and scanned. The water was subsequently replaced by 1000mL of mineral oil (ρ = 0.84 g/cm^3) and the tomographic scan process repeated using a fresh sheet of unexposed radiochromic film. To ensure adequate exposure of the radiochromic film using the low flux CT scanning technique, each film dosimeter was exposed to three consecutive full tomographic scans under each experimental setup and the dosimeter responses were scaled to represent a single scan measurement.

Figure 3 shows grayscale images of the absorbed dose to the conical breast phantom in water and oil, measured using the radiochromic film. Also shown in Figure 3 are horizontal (#1-3) and vertical (#4) profiles that illustrate the variation in dose at different distances from the 'chest wall' of the phantom to the 'nipple'. The mean cumulative dose measured in the 2D conical cross section of the water-filled conical phantom was 5.3 ± 0.6mGy, and that of the oil-filled phantom was 3.1 ± 0.3mGy. The profiles indicate that the measured dose in water was consistently greater than that of the equivalent profile in oil for all positions. This was attributed to the greater mass energy absorption coefficient of water compared to oil at 36keV, used to mimic glandular and fatty tissue, respectively. There was a pronounced concavity in the water dose profile at the thickest section of the phantom (profile #1 in Figure 3) with an approximate 50% difference between the peak periphery measured dose (~6mGy) and the center of the phantom (~4mGy). Horizontal dose profiles progressively flattened closer to the nipple (see profile #2, Figure 8, generated at a 9.25cm diameter, and 5cm from the 'chest wall'), due to the decrease in effective phantom diameter. As the breast diameter further decreases, the cumulative absorbed dose in the center of the breast, aggregated over the tomographic scan, increasingly approaches that of the entrance, or 'skin' dose. Indeed, the convex appearance of profile #3 (see Figure 3, generated at a diameter of approximately 3cm, and 10cm from the 'chest wall'), indicates that very close to the nipple, the center of the phantom cumulatively absorbs more dose than the skin.

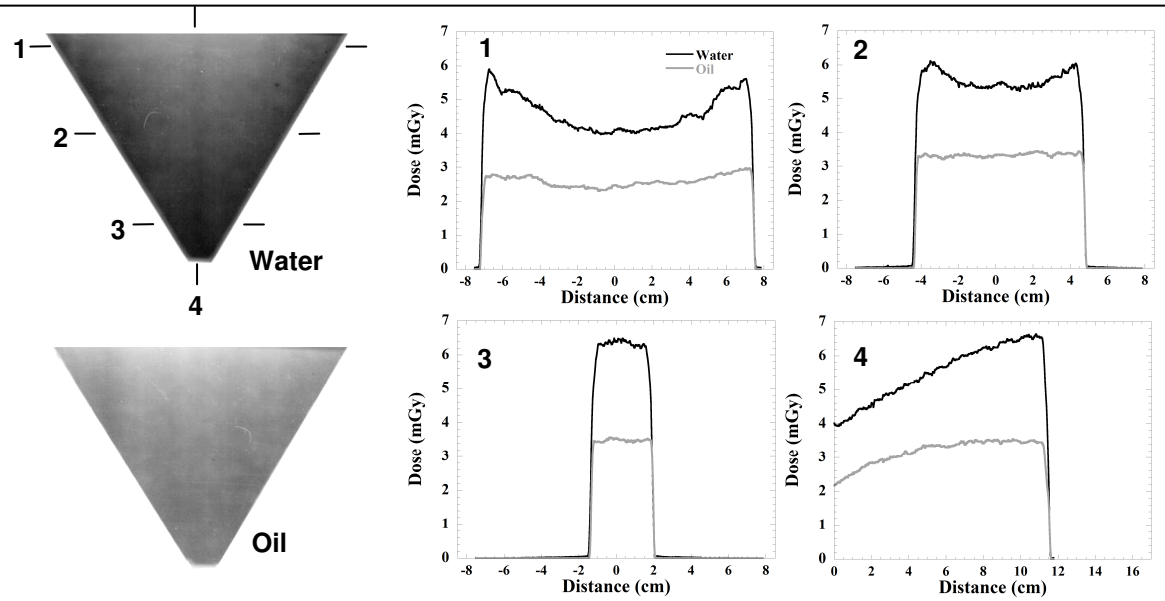

Figure 3 (Left**)** Grayscale images of the absorbed dose in the water- and oil-filled conical phantom as measured by the radiochromic film, with (Right) accompanying horizontal (#1-3), and vertical (#4) profiles. Note the pronounced concave dose profile across the thickest section (profile #1, 'chest wall') of the cone, becoming less pronounced (profile #2) and turning convex as the effective diameter of the conical volume decreases near the nipple (profile #3). Note also that the mean dose level increases closer to the nipple (profile #4). The >50% increase in dose between the chest wall and nipple is evidence of the influence that the breast diameter has on absorbed dose.

The increasing nature of the vertical profile (#4) in going from the chest wall towards the nipple illustrates the increasing overall dose with decreasing phantom diameter. The dose measured along the medial section of the phantom increased from 4mGy at the chest wall to approximately 6.5mGy by the nipple region (see profile #4 in Figure 3). These results show that, similar to mammography where a uniformly compressed breast is imaged, different sections of the uncompressed breast may absorb different amounts of radiation during a tomographic breast scan, in this case upwards of 65% more in certain areas close to the nipple. This result is instructive for dedicated breast imaging system design going forward.

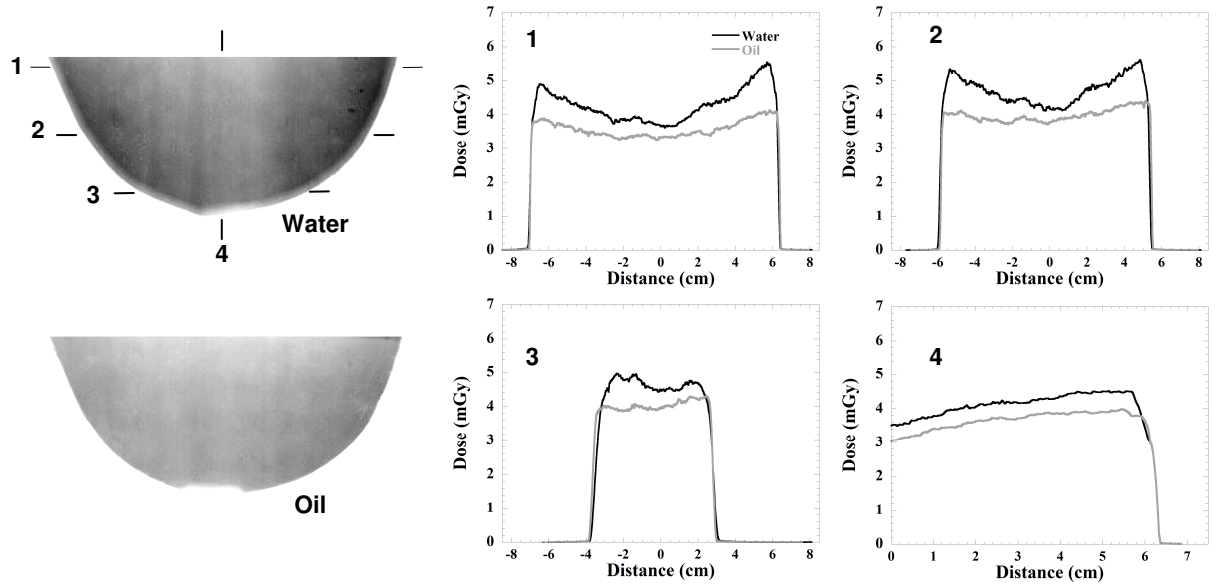

Figure 4 (Left) Grayscale images of the absorbed dose in the water- and oil-filled anthropomorphic phantom measured by the radiochromic film with (Right) accompanying horizontal (#1-3) and vertical (#4) profiles. Similar to the responses observed in the conical phantom, the horizontal dose profiles progressively flatten and the mean dose level increases approaching the nipple. . The vertical dose profile (#4) indicates a 28% increase in dose along the center of the breast from the chest wall towards the nipple.

Figure 4 illustrates grayscale images of the dose measured in the more clinically relevant anthropomorphic breast phantom. The mean dose measured in the water-filled phantom was 4.5 ± 0.4mGy and that of the oil-filled volume is 3.8 ± 0.2mGy. Similar to the conical shape, the results in Figure 4 also illustrate an increase in mean dose levels closer to the nipple. Evident in the profiles is the cupping close to the chest wall of the breast (profile #1 is generated at a breast diameter of 13.4cm, and a distance of 0.5cm from the 'chest wall') and the gradual flattening of the profile as the nipple is approached. However, the anthropomorphic breast does not taper near the nipple as sharply as the cone (the breast diameter for profile #3 is 6cm, at a distance of 7cm from the chest wall) and so the convex-shaped profile that was present close to the nipple in the conical phantom is not present in the anthropomorphic breast phantom.

Histograms of dose values from the radiochromic films (Figure 5, left) acquired across the 2D cross sections of both the oil- and water-filled anthropomorphic breast phantoms show a broader spectrum of dose values for the water-filled phantom. There is a slight skew towards the higher dose levels in water, whereas dose in the oil filled phantom is more tightly distributed about the mean, illustrating the more uniform distribution of the dose figures for the oil filled phantom.

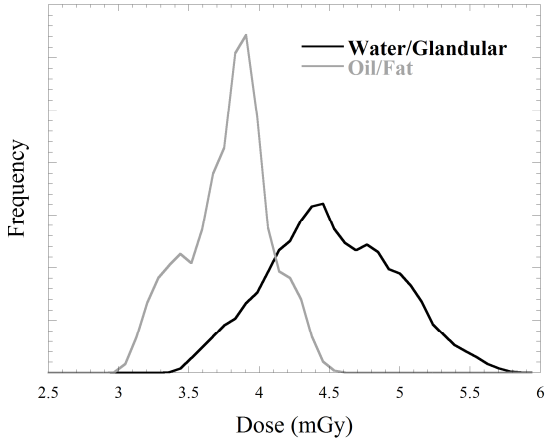

Figure 5 Area normalized histogram of dose measurements for the anthropomorphic breast volume filled with water (black) and oil (light gray). The histograms illustrate the broader distribution of dose in the more glandular breast tissue compared to the fatty tissue.

Unlisted Task: Measure the dose in a cadaveric uncompressed breast

A cadaver breast, obtained from a 48-year old woman who died of causes other than breast cancer, was also used to investigate the dose to uncompressed human breast tissue using the standard tomographic protocol used with the breast CT system.

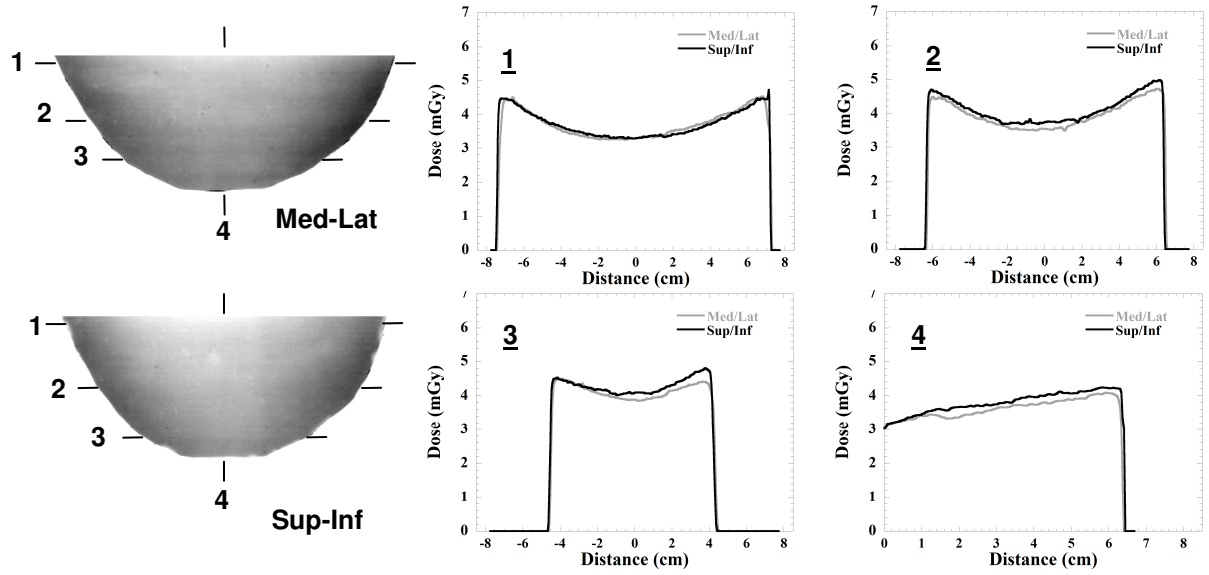

Figure 6 Grayscale images of the absorbed dose in the cadaver breast for the medial-lateral and superior-inferior film templates. The accompanying dose profiles indicate good agreement for the templates across dose profiles as the nipple is approached.

The breast was cut initially along the medial-transverse breast dimension from posterior to anterior breast. A sheet of radiochromic film, cut to the contoured template of the breast phantom cross-section, was inserted between the two cut sections of breast tissue. Due to the lack of an attached chest wall, the excised breast volume tended to sag in the middle of the phantom and so 175mL of mineral oil was added to ensure a continuum of tissue equivalent medium above the chest wall of the suspended breast. To provide a form of

self-validation of the results, the entire experimental protocol was repeated using a new sheet of radiochromic film inserted into an incision cut orthogonally into the suspended breast along the medial-sagittal dimension.

The overall mean doses measured for the cadaver tissue, measured outside of the oil-filled regions, were 4.3 ± 0.3mGy and 4.2 ± 0.3mGy in the medial-lateral (transverse) and superior-inferior (sagittal) directions, respectively. The measured dose ranges from 3.3 to 5.1mGy across both cadaver film orientations (see Figure 6).These breast tissue dose measurements are between the mean doses of 3.8 ± 0.2mGy and 4.5 ± 0.4mGy measured for the oil and water-filled phantoms, respectively.

Figure 7 illustrates a composite histogram of the dose distribution of the cadaver breast tissue and those of the oil and water-filled anthropomorphic phantoms. The histogram indicated that the dose distribution in the cadaver breast tissue, composed primarily of adipose and glandular tissue among others was, as expected, located between the dose distributions of the oil and water filled anthropomorphic phantom data. This result validated the previous anthropomorphic data using the boundary materials of oil and water to simulate lower and upper material composition bounds. Table 1 summarizes the measured dose results across all the various setups and illustrates the trends found in the dose figures, especially as a function of the oil (O) and water (W) filled phantoms.

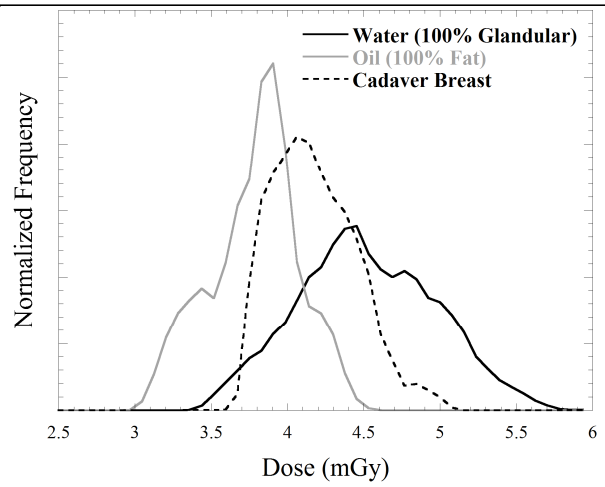

Figure 7 Histogram composed of the (black) water and (light gray) oil-filled anthropomorphic breast phantom dose distribution along with the dose distribution of the combined cadaver breast tissue measurements (dark gray). The cadaver dose histogram has been averaged across both orientations of the film.

Table 1. Mean and standard deviation (SD) dose for the various investigated setups..

			Mean Dose (mGy)	±SD Dose (mGy)
Phantom	Cylinder	(W)	5.4	0.4
		(O)	3.5	0.3
	Cone	(W)	5.6	0.3
		(O)	3.1	0.3
	Anthro.	(W)	4.5	0.4
		(O)	3.8	0.2
Cadaver Breast			4.3	0.3

Task 3:

Task 3(a): Design and manufacture a new physical gantry for the CmT system that supports full 3-D motion

Due to last minute funding circumstances outside of the control of the PI, it was not possible to manufacture the fully flexible 3D CmT system as proposed in the Statement of Work. However, a new fully flexible 3D design was created which will form the basis for future system design iterations. Because of the reduced funding it was not possible to implement Task 4 of the original Statement of Work.

The next generation design, shown in Figure 8, consists of the same x-ray tube and detector that is now capable of controlled movement around both a vertical and a horizontal axis of rotation. In the proposed new design, the horizontal rotation is controlled as before but the vertical rotation is completed using a new liner motor that travels down a track with great accuracy. The translation of the motor on its linear track has the effect of pulling and pushing the new gantry in a see-saw like fashion about the isocenter of the CmT system, enabling the system to tilt around the envelope of a hemi-sphere located at the isocenter, with radius equal to the isocenter to detector distance of the new CmT system. The concept system design is shown in Figure 8 using accurately modeled computer aided design models.

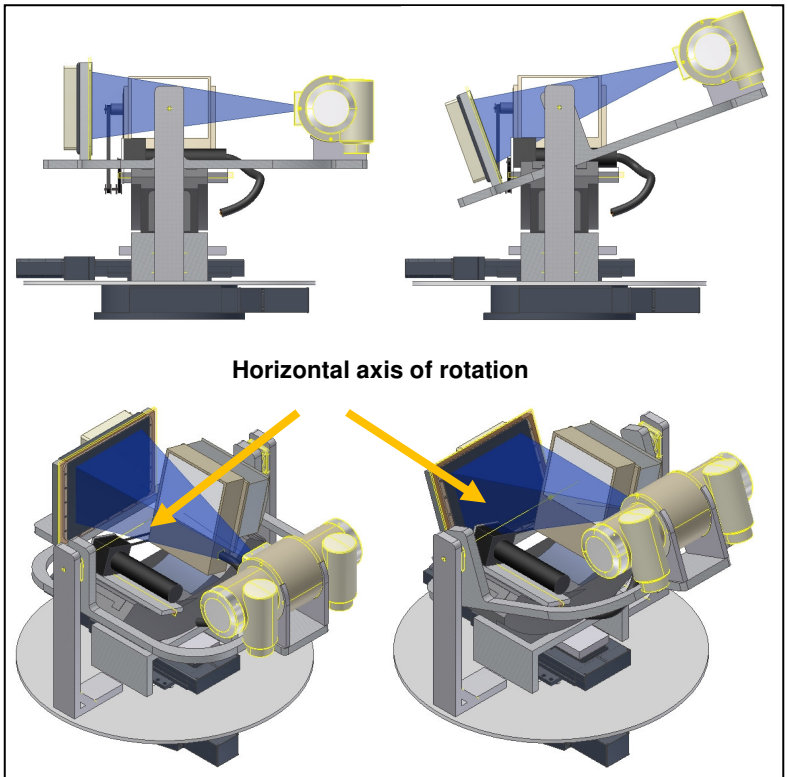

Figure 8: CAD concept designs from side-on and oblique perspectives of a next generation integrated SPECT-CmT system. The concept includes a CmT system that can tilt in the polar direction via a see-saw type mechanism about a horizontal axis of rotation through the isocenter of the CT system.

and narrow-edge detector with a blue cone beam.

Task 3(d): Integrate the new CmT positioning system with the existing SPECT subsystem

The existing SPECT system is also shown integrated with the new CmT system and positioned orthogonally to the CmT system. There is enough clearance designed into the positioning of the SPECT system to enable fully integrated and simultaneous or interleaved imaging of the pendant breast of the patient.

Task 3(c). Design and manufacture a new comfortable radio-opaque patient bed to allow full 3-D motion of both imaging subsystems positioned below the bed.

A bed was also designed in CAD, again not manufactured, that would accommodate the movement of the newly integrated and fully 3D SPECT and CmT systems to image the breast of the patient. The design, shown in Figure 9, consists of contoured section towards the mid-torso and head of the patient that would allow comfortable prone positioning of the patient. The reduced width of the system at the head section is also designed to allow the CmT system, in particular, to tilt in the polar direction. Figure 9 illustrates the bed with a new end-on x-ray tube

As of this writing, the new integrated and fully 3D CmT and SPECT system has not yet been implemented, although it is hoped that funding for the project will be applied to the design in the near future, ultimately resulting in improved volumetric imaging of the breast and chest wall.

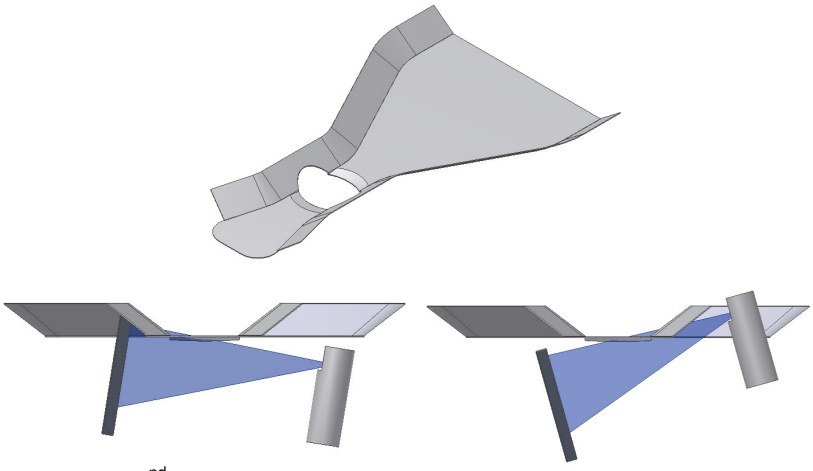

Figure 9: Concept design of a 2nd generation bed to allow a narrow edge detector and end-on x-ray tube to tilt in the polar direction. This will enable improved cone beam image quality and increase the imaged volume of breast tissue. The bed is shown (top) from an oblique angle above the bed and (bottom) from a front-on perspective, with a unipolar tube and narrow edge detector tilting the cone beam field of view in the polar direction.

Task 5:

Task 5(b). Prepare and submit research work to peer-reviewed journals.

A manuscript detailing the breast dosimetry study was submitted to Medical Physics. That manuscript is in revision and will be resubmitted soon, to be published this year.

Task 5(c). Attend and present at local seminars offered at Duke University through Medical Physics and the Breast and Ovarian Oncology Research Program.

The breast dosimetry study was presented at the annual Duke Comprehensive Cancer Center meeting in February 2010.

Task 5(d). Attend international conferences such as SPIE Medical Imaging Conference, DOD BCRP Era of Hope Meeting, IEEE Medical Imaging Conference, RSNA Conference, and San Antonio Breast Cancer Symposium.

The dosimetry study was presented orally at the SPIE Medical Imaging Conference in San Diego, California in February 2010. The manuscript accompanying the presentation was a finalist in the Michael B. Merikel Student Paper award.

Task 5(e). Prepare thesis and defend.

The thesis detailing the author's combined efforts over the course of his graduate studies at Duke was prepared over the course of 6 months and successfully defended in March 2010.

C. KEY RESEARCH ACCOMPLISHMENTS

Year 2 included Task 1(a), and Task 4(a), (c), and (d).

- Measured the dose absorbed by the uncompressed breast during a regular CT scan acquired using our quasi-monochromatic dedicated breast imaging device. This dose was acquired using a relatively new radiochromic film technique, for breast imaging, validated by the use of TLDs.
- Designed in software, the next generation integrated SPECT-CmT breast cancer imaging device that incorporates fully 3D SPECT and CT devices.
- Designed the next generation patient bed for prone patient imaging using the new integrated SPECT-CmT imaging device.
- Presented research at local and international research conferences, including the Duke University Comprehensive Cancer Center annual meeting, and the 2010 SPIE Medical Imaging Conference.
- Was a finalist in the Michael B. Merickel Student Paper Award at the 2010 SPIE Medical Imaging Conference.
- Submitted manuscript to Medical Physics which is now in revision for resubmission and potential acceptance for publication.
- Prepared and successfully defended my doctoral thesis.

D. REPORTABLE OUTCOMES

Peer Reviewed Papers

D.J. Crotty, S.L. Brady, D.C. Jackson, G.I. Toncheva, C.E. Anderson, T.T. Yoshizumi M.P. Tornai "Measurement of the absorbed dose in the breast using a dedicated CT mammotomography system employing a quasi-monochromatic x-ray beam and radiochromatic film". Submitted to Medical Physics, (currently in revision)

Conference Proceedings and Presentations

D.J. Crotty, S.L. Brady, D.C. Jackson, G.I. Toncheva, C.E. Anderson, T.T. Yoshizumi M.P. Tornai "Investigating the dose distribution in the uncompressed breast with a dedicated CT mammotomography system". Presented at the 2010 SPIE Medical Imaging Conference, San Diego, CA, Feb 2010 and published in the 2010 Proceedings of the SPIE Medical Imaging Conference

D.J. Crotty, D.C. Jackson, S.L. Brady, G.I. Toncheva, C.E. Anderson, T.T. Yoshizumi, M.P. Tornai. "Empirical measurement of the 3D dose distribution in the uncompressed breast using a dedicated CT mammotomography system". Presented at the 2010 Duke University Comprehensive Cancer Center Annual Meeting.

D.J. Crotty, D.C. Jackson, S.L. Brady, G.I. Toncheva, C.E. Anderson, T.T. Yoshizumi, M.P. Tornai. "Empirical Measurement of the 3D Dose Distribution in the Uncompressed Breast Using a Dedicated CT Mammotomography System." Presented at the *2009 Annual Meeting of the Duke Comprehensive Cancer Center*, 5 October 2009, Durham, NC, p. 35.

M.P. Tornai, R.L. McKinley, **D.J. Crotty**, S.J. Cutler, P. Madhav, K.L. Perez. "Breast Imaging Devices for Screening, Diagnostics and Treatment Monitoring." Presented at *Clinical Directions for Molecular Imaging*, Duke University, Durham, NC.

E. CONCLUSION

Research in Year 2 was dominated by the extensive dosimetry study into the absorbed dose during a dedicated breast CT scan. Using a radiochromic film technique and a cadaveric breast specimen, it was found that the breast absorbs approximately 4.2mGy during a scan using the current dedicated breast imaging device. It was also found that the point breast doses vary depending on the shape of the breast and the relative location of the region of interest within the pendant breast volume. A next generation combined SPECT-CmT device was designed, the major concepts of which will be implemented in the new design iteration of the device design. A new patient bed was also designed to enable fully 3D SPECT and CT imaging of the prone patient's pendant breast. Research was presented at several local and international research conferences, and an educational site visit was undertaken to Varian. A manuscript was submitted to a peer-reviewed journal that is currently in revision and a doctoral thesis was successfully prepared and defended.

F. REFERENCES

[1]D. J. Crotty, R. L. McKinley, P. Madhav, S. J. Cutler and M. P. Tornai, presented at the Medical Imaging 2009: Physics of Medical Imaging, Lake Buena Vista, FL, USA, 2009 (unpublished).

[2]P. Madhav, S. J. Cutler, D. C. Crotty, K. L. Perez, R. L. McKinley, L. Wilke, T. Wong and M. P. Tornai, "Pilot Patient Studies Using a Dedicated Dual-Modality SPECT-CT System for Breast Imaging " 2008 AAPM (2008).

[3]M. J. Butson, P. K. N. Yu, T. Cheung and P. Metcalfe, "Radiochromic film for medical radiation dosimetry," Materials Science and Engineering: R: Reports **41**, 61-120 (2003).

[4]S. Devic, J. Seuntjens, E. Sham, E. B. Podgorsak, C. R. Schmidtlein, A. S. Kirov and C. G. Soares, "Precise radiochromic film dosimetry using a flat-bed document scanner," Med Phys **32**, 2245-2253 (2005).

[5]S. Devic, N. Tomic, Z. Pang, J. Seuntjens, E. B. Podgorsak and C. G. Soares, "Absorption spectroscopy of EBT model GAFCHROMIC film," Med Phys **34**, 112-118 (2007).

[6]L. Bassett, C. D'Orsi, C. Lee, P. Butler, R. Jong and B. Monsees, "Practice guidelines for the performance of screening and diagnostic mammography," (2008).

[7]J. M. Boone, "Glandular breast does for monoenergetic and high-energy X-ray beams: Monte Carlo assessment," Radiology **213**, 23-37 (1999).

[8]P. Russo, T. Coppola, G. Mettivier, M. C. Montesi and A. Lauria, "Distribution of Absorbed Dose in Cone-Beam Breast Computed Tomography with Radiochromic Films," IEEE Nuclear Science Symosium and Medical Imaging (2009).

[9]P. Russo, A. Lauria, G. Mettivier and M. C. Montesi, "Dose distribution in cone-beam breast computed tomography: An experimental phantom study," IEEE Nuclear Science Symposium Conference Record, 5623-5628 (2008).

[10]J. M. Boone, "Normalized glandular dose (DgN) coefficients for arbitrary x-ray spectra in mammography: Computer-fit values of Monte Carlo derived data," Medical Physics **29**, 869-875 (2002).

[11]J. M. Boone, T. R. Nelson, K. K. Lindfors and J. A. Siebert, "Dedicated breast CT: radiation dose and image quality evaluation," Radiology **221**, 657-667 (2001).

APPENDIX A: ORIGINAL STATEMENT OF WORK

Task 1: Optimize tradeoffs between absorbed dose and image quality for the CmT subsystem:
a. Embed thermoluminescent dosimeters or available MOSFET detectors in anthropomorphic breast phantoms to evaluate dose for various sizes and compositions of breast equivalent tissue and lesions.
b. Use quantitative measures of image quality such as SNR, contrast, dose efficiency, and attenuation coefficient accuracy to correlate trends in image quality as a function of measured dose to the breast.
c. Qualitative metrics to describe observable artifacts will also be used to assess trends in image quality with absorbed dose.

Task 2: Investigate the effect on image quality of the limited 3-D motion of the current prototype dual-modality imaging system:
a. Integrate the existing prototype dual-modality imaging system with the new custom designed patient bed system.
b. Use various geometric and anthropomorphic breast phantoms with embedded lesions to quantify standard image quality metrics from images reconstructed using limited tomographic acquisition for both SPECT and CmT. Objective measures of image quality described in Task 1 will again be used to assess the performance of the system.

Task 3: Implement synchronized 3-D positioning and data acquisition for the prototype dual-modality imaging system:
a. Design and manufacture a new physical gantry for the CmT system that supports full 3-D motion.
b. Modify existing software programs to fully synchronize the 3-D motion and data acquisition of both the SPECT and CmT subsystems.
c. Design and manufacture a new comfortable radio-opaque patient bed to allow full 3-D motion of both imaging subsystems positioned below the bed.
d. Integrate the new CmT positioning system with the existing SPECT subsystem.
e. Quantify the effects of this improved 3-D positioning capability on image quality metrics equivalent to those outlined in Task 2.

Task 4: Evaluate and compare performance of the fully 3-D SPECT-CmT system to Mammography and Scintimammography:
a. Utilize an available breast phantoms containing various dual modality lesions to acquire 2-D planar data under varying compressions for scintimammography and mammography as well as uncompressed breast 3-D dual-modality tomographic imaging.
b. Conduct an observer study to compare mammography and scintimammography with dual-modality imaging for smallest lesion detectability in reconstructed images of breast phantoms under various operating parameters.

Task 5: Complete other aspects of the breast cancer training program:
a. Shadow a radiologist(s) to observe the clinical and diagnostic side in breast cancer imaging (Nuclear Medicine, Mammography).
b. Prepare and submit research work to peer-reviewed journals.
c. Attend and present at local seminars offered at Duke University through Medical Physics and the Breast and Ovarian Oncology Research Program.
d. Attend international conferences such as SPIE Medical Imaging Conference, DOD BCRP Era of Hope Meeting, IEEE Medical Imaging Conference, RSNA Conference, and San Antonio Breast Cancer Symposium.
e. Prepare thesis and defend.

APPENDIX B: Abstract for the Duke Comprehensive Cancer Center Meeting, Feb. 2010

Empirical measurement of the 3D dose distribution in the uncompressed breast using a dedicated CT mammotomography system

Dominic J. Crotty,[1,2] D'Vone C. Jackson,[1,3] Samuel L. Brady,[1,3,4] Greta I. Toncheva,[1,4] Colin E. Anderson,[1,4] Terry T. Yoshizumi,[1,3,4] Martin P. Tornai[1,2,3]

[1]*Department of Radiology, Duke University Medical Center, Durham, NC 27710*
[2]*Department of Biomedical Engineering, Duke University, Durham, NC 27708*
[3]*Duke University Medical Physics Graduate Program, Durham, NC 27710*
[4]*Radiation Safety Division, Duke University Health System,* Durham, NC 27710

A prototype integrated dual modality SPECT-CT system designed for uncompressed tomographic molecular-anatomic breast imaging has been developed. The CT subsystem incorporates an innovative ultra-thick K-edge x-ray filtration technique that optimizes the system's dose efficiency (SNR^2/dose) for lesion imaging. Dosimetric analysis of breast x-ray CT systems is typically performed through physical measurement in air, computer modeling of the energy-dependent spectra and tracking the energy deposition in voxelized phantoms using simulation code. Here, we directly measure the full-3D uncompressed breast dose under our standard tomographic cone beam CT imaging protocol using ionization chamber-calibrated thermo-luminescent dosimeters and radiochromic film. Two geometric phantoms and an anthropomorphic breast phantom are filled in turn with 1L of water and oil simulating the effective density bounds of 100% glandular and fatty breast compositions, respectively. Volumetric dose measurements across the different breast equivalent materials and phantom shapes are generated. Point doses to the water-filled geometric and anthropomorphic breast phantoms for a single complete tomographic scan range from 1.3-7.3 mGy and 1.7-6.3 mGy, respectively, with a mean whole-breast dose of 4.5 mGy. This mean value for a fully-3D image is equal to that for standard 2-dimensional x-ray mammography. Trends indicate lower doses in the centers of the volumes and the posterior "breast" towards the chest wall along with higher doses near the nipple regions. Measured doses to the oil-filled phantoms are less due to the smaller mass energy-absorption coefficient of oil relative to water. These results completely characterize the 3D dose distributions in various shaped volumes in a dedicated breast imaging paradigm, and confirm the advantages of using the novel ultra-thick K-edge beam to minimize the dose to the breast during fully-3D imaging. This study is the first that we are aware of to physically measure the 3D dose distribution to the breast from a dedicated breast CT system.

APPENDIX C: 2010 SPIE Medical Imaging Conference Proceedings/Student Paper Award Finalist

Investigating the dose distribution in the uncompressed breast with a dedicated CT mammotomography system

Dominic J. Crotty,*[a,b] Samuel L. Brady,[a,c,d], D'Vone C. Jackson,[a,c] Greta I. Toncheva,[a,d] Colin E. Anderson,[c,d] Terry T. Yoshizumi,[a,c,d] Martin P. Tornai[a,b,c]

[a]*Department of Radiology, Duke University Medical Center, Durham, NC 27710*
[b]*Department of Biomedical Engineering, Duke University, Durham, NC 27708*
[c]*Duke University Medical Physics Graduate Program, Durham, NC 27710*
[d]*Radiation Safety Division, Duke University Health System,* Durham, NC 27710

Abstract

A dual modality SPECT-CT prototype system dedicated to uncompressed breast imaging (mammotomography) has been developed. The CT subsystem incorporates an ultra-thick K-edge filtration technique producing a quasi-monochromatic x-ray cone beam to optimize the dose efficiency for uncompressed breast tomography. We characterize the absorbed dose to the breast under normal tomographic cone beam image acquisition protocols using both TLD measurements and ionization chamber-calibrated radiochromic film. Geometric and anthropomorphic breast phantoms are filled with 1000mL of water and oil to simulate different breast compositions and varying object shapes having density bounds of 100% glandular and fatty breast compositions, respectively. Doses to the water filled geometric and anthropomorphic breast phantoms for a tomographic scan range from 1.3-7.3mGy and 1.7-6.3mGy, respectively, with a mean whole-breast dose of 4.5mGy for water. Measured trends in dose distribution indicate lower doses in the center of the breast phantoms towards the chest wall along with higher doses near the peripheries and nipple regions. Measured doses to the oil-filled phantoms are consistently lower across all volume shapes (mean dose, 3.8mGy for the anthropomorphic breast). Results agree with previous Monte Carlo dose estimates generated for uncompressed breast imaging and illustrate the advantages of using the novel K-edge filtered beam to minimize breast dose during fully-3D imaging.

1. Introduction

A few research groups, including ours, have developed prototype devices dedicated to breast cancer imaging using cone beam computed tomography (breast CT or mammotomography)[1]. One advantage of these tomographic devices over dual view mammography, the current standard of care for breast cancer screening, is the potential for improving contrast between tissues with similar attenuation coefficients in reconstructed images of the breast volume. By improving visibility of small lesions that may otherwise remain occluded in conventional 2D planar imaging using mammography, 3D volumetric imaging using a dedicated CT system may improve the diagnostic accuracy of breast imaging, increase the effectiveness of breast cancer screening and consequently have a significant positive impact on patient outcomes.

Since breast CT acquires many hundreds of individual 2D projection images, the cumulative dose absorbed by the breast during a tomographic scan is of paramount importance to imaging system design[2]. Guidelines from the American College of Radiology (ACR) require that the average absorbed dose from dual view mammography to a 4.2cm-thick compressed breast consisting of 50-50% adipose-glandular tissue not exceed 6mGy[3]. Lacking an equivalent standard for uncompressed breast imaging since the technology is still in its infancy, investigators likewise aim to confine the cumulative absorbed dose for a breast CT scan to that around dual view mammography as a starting point in system development and optimization.

Dosimetry for mammography has been performed using both empirical and simulation-based measurements[4-8], whereas dosimetry for breast CT has generally been estimated using a combination of measurements in air, computer-modeling of x-ray tube spectra incident on the breast, and validated Monte Carlo simulations [9-10].

Initial Monte-Carlo-based dosimetry studies demonstrated the ability of breast CT to successfully image the uncompressed breast at doses equivalent to that of mammography[11-12]. Two subsequent studies generated dose conversion factors specifically for breast CT as a function of various imaging techniques and breast compositions [9-10]. In addition to generating the conversion factors and additionally estimating the cumulative absolute dose to simulated uncompressed breasts, the studies also simulated the spatial dose distribution for breast CT at different beam energies and tube potentials. One study[10], using mean beam energies of 20-40keV in the simulated system, similar to those employed in the practical system described in this study, showed that the resulting dose profiles across the breast phantom were highly non-uniform, with dose absorbed at the periphery of the phantom being far higher than in the center . Horizontal dose profiles across the phantom were shown to become more uniform as the simulated mean beam energy increased above approximately 60keV. In a different study[9] using tungsten tube potentials from 80-120kVp, a much more uniform dose profile for breast CT was demonstrated at these higher tube potentials. A recent study[13] employed embedded TLDs to study the dose distribution in a 14-cm diameter PMMA half-ellipsoid phantom. By varying tungsten target x-ray tube potentials from 60-80kVp, the dose was seen to increase appreciably towards the periphery both in the radial (towards the skin) and axial (towards the anterior breast). However, a more recent followup study by the same investigators using radiochromic film and the same imaging system at 80kVp indicated a fall off in dose towards the nipple[14].

The prototype breast CT imaging system described in this work, developed as part of a novel prototype dual modality SPECT-CT system for uncompressed breast imaging, has recently been used to image human subjects with encouraging results[2, 15-16]. When previously compared against dual view mammography in a phantom-based observer study, this CT subsystem demonstrated improved ability to visualize small (<5mm) spherical 'lesions' in low-contrast images containing structured background material at doses comparable to that of dual view mammography [17]. In that observer study, the dose imparted to the breast from breast CT was estimated using the dose conversion factors previously defined[9] no experimental validation of the absolute dose estimates was available.

In contrast to previous simulation studies, this study empirically quantifies the dose imparted to the breast and illustrates the spatial dose distribution obtained using our dedicated breast CT imaging system. We characterize the absorbed dose to the uncompressed breast using a standard tomographic cone beam imaging protocol in conjunction with calibrated thermoluminescent dosimeters (TLDs) and ionization chamber-calibrated radiochromic film Two separate absorptive scatter media are employed in the breast phantom volume to illustrate the variation in absorbed dose for what would be expected boundary conditions of 100% adipose or 100% glandular breast tissue composition, though it is anticipated that no such boundary may actually exist [18]. Finally, three different phantom shapes are tested to observe variations in absorbed breast dose as a function of the shape and effective radius of the breast phantoms and x-ray cone beam intersecting it. As far as we are aware, this is the first empirical study undertaken of the 3D dose distribution inside breast phantom volumes using a dedicated breast imaging system, TLDs, radiochromic film, and in media that mimic the boundary value characteristics of breast tissues.

2. Materials and Methods

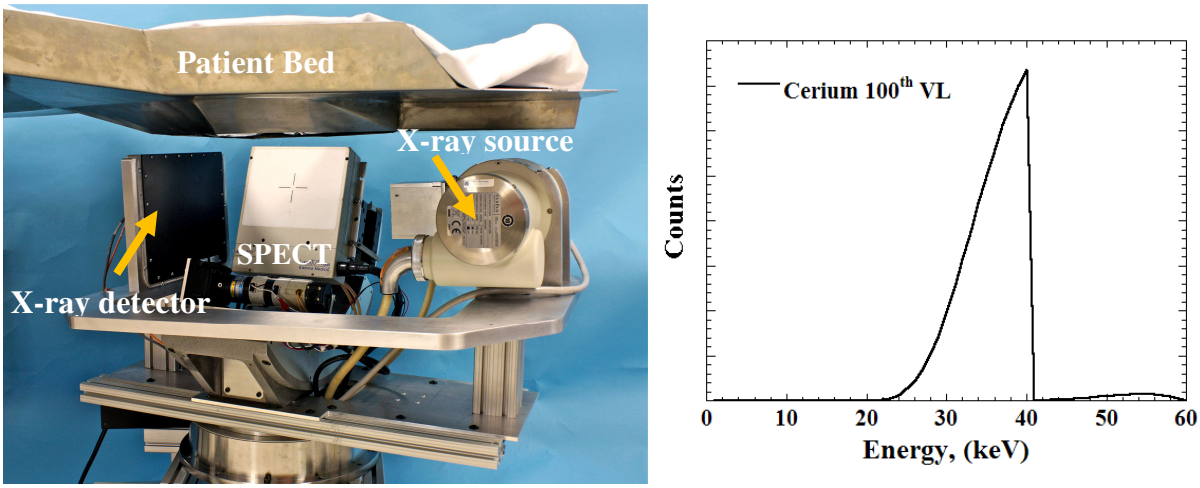

Figure 1 (Left) Photograph of the prototype integrated SPECT-CT system dedicated to breast cancer imaging rotating below the Pb-shielded patient bed. The SPECT system gamma camera is visible in the center of the image. The x-ray source and detector are nominally tilted from the horizontal. The combined system rotates around a vertical axis of rotation with the CT subsystem restricted to purely circular orbits in this prototype. (Right) Breast incident energy spectrum of the unconventional, ultra thick K-edge Ce-filtered beam at 60kVp].

2.1. Instrumentation

Details of the prototype compact dual-modality breast imaging system (Figure 1) are described elsewhere [16]. The SPECT and CT sub-systems are secured to a common rotation stage capable of 360° azimuthal rotations around the vertical chest to nipple axis of the pendant breast. The CT subsystem employs a rotating tungsten target cone-beam x-ray source (model Rad-94, 0.4mm focal size, 14° anode angle, *Varian Medical Systems*, Salt Lake City, UT) and a CsI:T1 based amorphous silicon digital x-ray detector (model *Paxscan* 2520, *Varian Medical Systems*, Salt Lake City, UT) with a grid size of 1920x1536 and 127μm pixel pitch. A cerium (Z=58, ρ=6.77g/cm^3, K-edge=40.4keV, *Santoku America, Inc.*, Tolleson, AZ) 100th value attenuating filter (0.0508cm, evaluated at 60kVp) is used to yield a mean x-ray beam energy of approximately 36keV and a FWHM of 15%[19-20] (Figure 1) . These non-conventional beam characteristics have been previously exploited to optimize the dose efficiency ([signal difference to noise ratio]^2/dose) of the system for uncompressed breast imaging[21]. For these studies, a 60cm source-to-image distance (SID) is used with a magnification of 1.57 for an object located at the system's center of rotation. The integrated CT sub-system is restricted to simple circular motion about a vertical axis at a nominal 3.11° fixed source-detector tilt to the horizontal. The typical tomographic data acquisition protocol consists of an x-ray exposure technique (60kVp, 100mA, 25msec) and 255 projection images collected about the breast; a number of the projection images are used for system calibration and other technical reasons.

2.2. *XRQA film preparation and readout*

The XRQA film (*International Specialty Products,* Wayne, NJ) used in the experiment undergoes solid-state polymerization in real time in reaction to incident radiation[22]. The polymerization creates a dye-complex darker in color compared to unexposed portions of the film, and is digitized after a 24 hour period needed to allow stabilization to occur. The polymerization in the film yields an absorption spectrum with a maximum at 635 nm [23], which is most sensitively detected with optical digitization using red light.

XRQA films were digitized using reflection densitometry[24-25] on a flatbed scanner (Expression 10000XL, *Epson America*, Long Beach, CA). The scanner employed a xenon gas fluorescent source light and a linear charged coupled device (CCD) array[26]for film readout. The scanner's source light illuminates only during previewing and scanning; so to "warm-up" the scanner, ten blank scans were performed in succession and then

discarded. Warming up the scanner provided a more stable light source and more consistent optical density (OD) readings[27]. The films were placed on the scanner in an area of high source-light uniformity; which corresponds to the center of the scanner. Each exposed film was scanned five times[27] at a resolution of 72 pixels/in (0.4 mm pixels), with no color corrections, and image files were saved in uncompressed format. All films were digitized using 48-bit color depth with RGB file format (16-bit per color channel) and the red (R) channel was extracted for analysis in Matlab (R2007a, *Mathworks Inc*., Natick, MA) [28]. The final image consisted of an average of the five scans smoothed with a 3x3 pixel kernel. The films were scanned prior to being exposed and then carefully realigned on the scanner for post-exposure scans (alignment error measured to be ~1mm). Once irradiated, the films darkened such that their OD quadratically increased with exposure [22, 29]. A net OD (netOD) [30] was calculated as the log transformation of the ratio of pre- (I_{pre}) and post-exposed (I_{post}) scanner light intensity value.

$$netOD = OD_{post} - OD_{pre} = \log_{10}\left(\frac{I_0}{I_{post}}\right) - \log_{10}\left(\frac{I_0}{I_{pre}}\right) = \log_{10}\left(\frac{I_{pre}}{I_{post}}\right)$$

where I_0 was the measured light intensity of the flat field scan performed at the same time of the pre- and post-exposure film scans.

2.3. TLD preparation and readout

All TLDs used in the experiment (3x3x1mm Harshaw TLD-100 (LiF:MgTi) chips, *Thermo Eberline, LLC*, Franklin MA) were first tested for batch uniformity by being exposed to a cumulative exposure of 1R. All chips that deviated greater than 2 standard deviations from the batch mean were discarded. The TLDs were annealed using a TLD-annealing furnace (168-300, *Radiation Products Design, Inc.*, Albertville, MN), and read using a TLD reader (Harshaw 5500, *Thermo Fisher Scientific, Inc*., Waltham, MA) with WinREMS software. Nitrogen gas was introduced during the readout cycle to reduce non-radiation-induced signals [31].

2.4. Dosimeter calibrations

The TLDs and XRQA film were cross-calibrated with a $6cm^3$ ionization chamber (Mammochamber, Model 10x5-6M-3, *RadCal*, Monrovia, CA). The ion chamber was calibrated by the University of Wisconsin's Accredited Dosimetry Calibration Laboratory. Four separate sets of dosimeters including one piece of film, two TLDs, and the ion chamber were exposed in air to four separate exposure levels with the quasi-monochromatic x-ray beam, ranging from 659.5mR to 1.915R. The dosimeters were located approximately 38cm from the x-ray focal spot (on the tomographic system's isocenter) and localized along a vertical line near the center of the x-ray cone beam field of view to eliminate variations associated with the heel effect due to the tube's orientation. One set of TLDs and one section of film were set aside elsewhere in the laboratory for background measurements. TLD and film responses were plotted as a function of the measured ion chamber exposure readings converted to absorbed dose. Absorbed dose was calculated by multiplying the ion chamber exposure reading by the energy dependent water and oil f-factors (0.88 cGy/R and 0.74 cGy/R, respectively for 36keV) and Wisconsin's provided calibration factor for 60 kVp. Both dosimeter calibration plots were fit using least-squares regression techniques.

2.5. Dose measurements of the breast phantom volumes using radiochromic film

Three breast phantom volumes were used to measure the absorbed dose to the breast using our CT system: two geometric phantoms in the shapes of a cylinder and a cone, and an anthropomorphically shaped breast phantom (Figure 2). The regular cylindrical phantom presents a constant cross section of absorbing material to the divergent x-ray cone beam, and mirrors the setup often used in Monte Carlo dose simulation studies. The

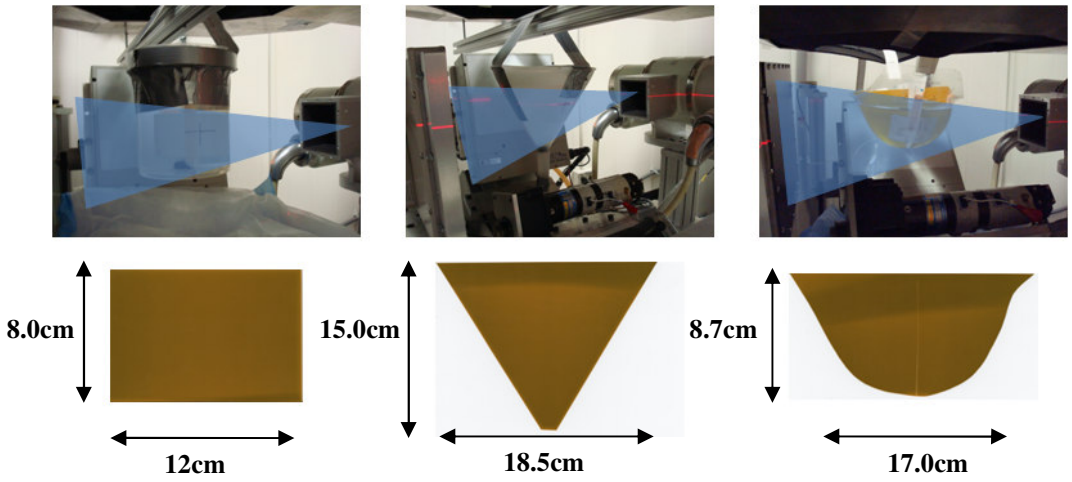

Figure 2 (Upper row) Photographs of the radiochromic film being scanned in (left) the cylindrical, (middle) conical and (right) anthropomorphic breast phantoms, respectively. A representation of the approximate position of the x-ray cone beam (blue polygon) emanating from the x-ray tube is superimposed over each setup. (Lower row) Photographs of the radiochromic film masks and their dimensions for the corresponding phantoms.

conical shape mimics the decreasing effective diameter of the pendant breast from chest wall to nipple, but does so in a controlled fashion. From previous studies [32] we have observed that approximately 15% of subjects have this conically shaped pendant breast. The anthropomorphic breast shape is then a natural progression from the prior geometric shapes and represents a 60% prevalent clinical geometric pendant breast dimension and volume [32].

Cross-sectional templates were cut out of the XRQA film of the phantom volumes (shown in Figure 2). With these given dimensions, the cone then simulates a large diameter breast at the upper edge of the cone, tapering to a smaller diameter breast towards the nipple. Due to the asymmetric 3D shape of the anthropomorphic breast phantom, separate templates of each axis (in sagittal and transverse orientations) were created by photographing the water-filled phantom from orthogonal perspectives. The orthogonal short axis film sections were sliced vertically through their centers to enable interlacing them.

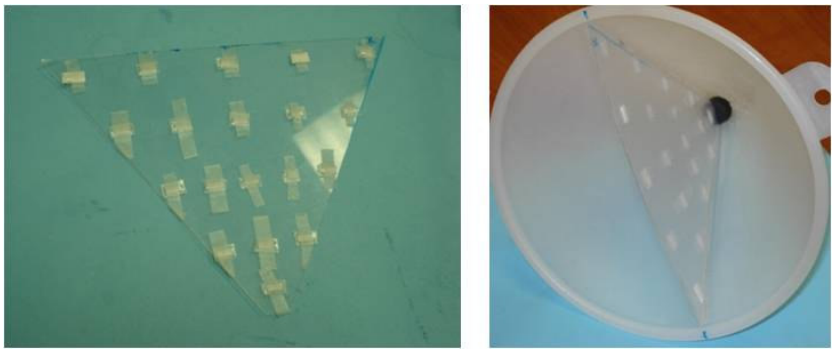

Figure 3 Photographs of the TLDs on (left) the template of the cone shaped container, and (right) in the cone breast phantom.

For each of the variously shaped phantoms, a single sheet of the film was attached with adhesive tape at several points to the inside surface of the phantom, ensuring minimal movement of the film during filling of the volumes with water or oil, and subsequent scanning. The phantoms were positioned at the isocenter of the cone beam CT imaging system (Figure 2), and scanned using the tomographic imaging protocol described previously. This enabled the absolute dose and dose profiles to be measured across the 2D central plane of each of the 3D breast phantom volumes. The phantoms were initially filled with 1000mL of water (ρ = 1.0 g/cm^3) and scanned. Using unexposed radiochromic film, the water was subsequently replaced by 1000mL of mineral oil (ρ = 0.84 g/cm^3) and the tomographic exposure process repeated. Water and oil were used to mimic the uniform tissue composition of breasts that form the boundaries of 100% glandular or adipose breast tissue composition, respectively. To ensure adequate exposure of the radiochromic film using the low flux CT scanning technique, each film dosimeter was exposed to three consecutive full tomographic scans under each experimental setup and the dosimeter responses were scaled to represent a single scan measurement

2.6. Validation of radiochromic film dose measurements using TLDs

Results from the radiochromic film measurements in the conical breast phantom were cross-validated with dose measurements acquired using TLDs. Thirty seven TLDs (18 pairs and 1 single TLD, with pairs being used to ensure greater accuracy in the "point dose" measurements) were located on a regular array of points across the triangular template of the conical phantom (Figure 3), to measure the dose to the breast at varying distances from the breast surface to the center of the breast, and at different anterior distances from the "chest wall" towards the decreasing diameter at the nipple. Each pair of TLDs was secured to a 5mm thin acrylic template of the conical phantom (Figure 3). The acrylic template and TLDs were then additionally vacuum-sealed to isolate the TLDs from liquid contamination, and to further secure them in place to the template surface. The entire TLD validation experiment was repeated twice, separated by a number of days to the first experiment (in case of local background differences) using identically located pairs of TLDs on the template. TLD data were pooled across the two separate measurements.

3. Results and Discussion

3.1. Dosimeter Calibration

Shown in Figure 4 are the quadratic fitting functions obtained for the calibration of the ionization chamber to the radiochromic film measurements in water and oil (R^2 = 0.99 in both cases), and the linear fitting functions for both calibration runs for the TLDs in water (R^2 = 0.99 in both cases). The fitting functions represented in Figure 4 were used to calibrate the XRQA film and TLDs measured *in situ* for the three phantoms. The shapes of these curves are consistent with the known characteristics of the dose-response of these dosimeters. Given that dosimetry with radiochromic film, especially immersed in fluids of different viscosity and density is still fairly new, the various measurements and appropriate least squares fits to the data can be used to calibrate one set of measurements from the other. In this case, the TLD and exposure meter measurements are considered the gold standard to which the radiochromic film is being calibrated and evaluated.

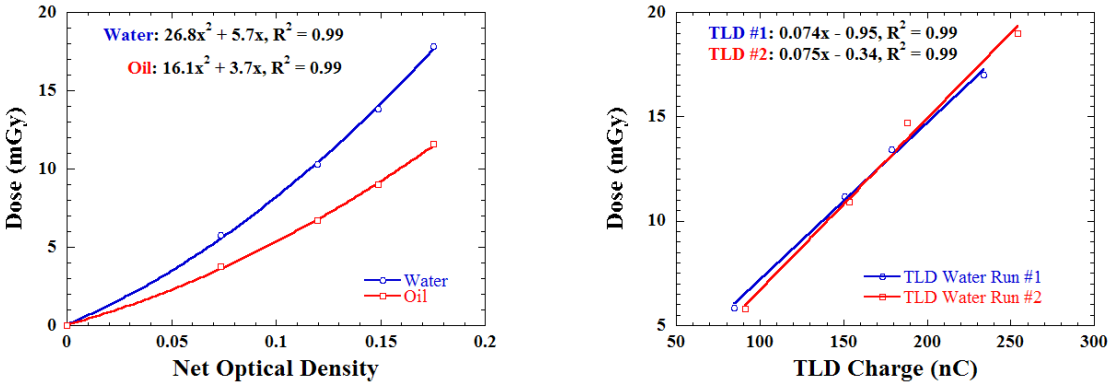

Figure 4 Calibration curves for absorbed dose as a function of (Left) radiochromic film optical density for water (blue) and oil (red) and (Right) generated TLD charge for water for both calibration runs. All calibrations show a close fit for the measured results.

3.2. Dose measurements

3.2.1. Cylindrical phantom

Figure 5 shows calibrated color plots of the absorbed dose to the cylindrical breast phantom in water and oil measured using the radiochromic film. Also shown in Figure 5 are horizontal and vertical profiles measured at different anterior distances from the 'chest wall' of the phantom to the 'nipple'. The profiles indicate that the measured dose in water is consistently greater than that of the equivalent profile in oil. This can be attributed to the greater mass energy absorption coefficient of water compared to oil at 36keV, used to mimic the coefficients for glandular tissue and fatty tissue, respectively. This difference in mean dose level between oil and water is consistent across all phantom shapes. The measured dose to the radiochromic film within the water filled cylindrical phantom for a single tomographic scan was measured to be 5.4 ± 0.4mGy, ranging from 3.4mGy to of 7.1mGy. The equivalent measurement for oil generated a mean dose to the oil filled phantom of 3.5 ± 0.3mGy with a range between 2.5 to 4.5mGy.

The horizontal dose profiles show a prominent cupping effect at the center of the cylinder for both water- and oil-filled phantoms. The measured cupping effect is similar to the cupping effects seen in others' simulation studies employing cylindrical phantoms at beam energies close to the mean beam energy of our breast CT system[10]. The cupping effect is not as prominent in the oil-filled phantom compared to the water-filled phantom. This is in part due to the greater mass energy absorption coefficient of water compared to oil at 36keV.

For the water phantom, peak dose levels at the periphery of the rectangular film are approximately 13% and 34% greater than at the center of the phantom for the left and right peripheries, respectively. The slightly increased horizontal asymmetry seen in the profiles may be primarily due to an uncentered cylinder that received a higher fluence while the CT system was on one side of the phantom. For oil, the dose profile is relatively flat from one periphery to the center of the cylinder but is approximately 20% higher than the center toward the other side. Given that the system obtains routine CT data with a full 360° scan, these sorts of asymmetries are expected to be minimal and appear to be impacted more due to greater breast density.

Other factors of the horizontal asymmetry were additionally interrogated. The measured variation in flat field light exposure across the calibrated radiochromic film scanner was approximately 1%, which effectively rules out bias in the scanning process. Some of the asymmetry may be caused by a larger number of "calibration

images" occurring at one specific azimuthal location of the cylinder relative to the x-ray source during the scan; however the effect of the proportionally small number of calibration exposures (4% of the total number of exposures are for calibration) cannot explain the magnitude of the elevated dose levels. Nevertheless, careful patient breast centering would be recommended given the close geometrical configuration of this compact system, and especially if the subject is suspected of having very dense breasts.

The vertical dose profile from chest wall to nipple demonstrates an approximate 5% change between maximum and minimum absorbed dose values. The greater uniformity in vertical dose profile may be due to the constant diameter that the cylinder presents to the divergent cone beam. If positioned exactly at isocenter, the constant diameter equalizes the path length of the x-rays incident on the cylinder and so photons tend to deposit the energy in a likewise consistent manner. There is a slight peak in the absorbed dose profile approximately where the central x-ray of the beam is located. This may be explained by two factors: the greater photon fluence (less divergence) near the central ray of the beam, progressively reducing towards the periphery of the beam; and, given the peaked 3D scatter-to-primary distribution in the center of cylinder [33], more scattered photons contribute to the dose in this symmetric cylindrical phantom. The greater decrease in dose levels towards the upper edge of the cylinder may be attributable to the proximity of the edge to the air interface where the lack of chest-wall scatter-in decreases the overall dose to the volume, especially when compared to the middle of the cylinder which is closer to the central ray of the beam.

3.2.2. Cone phantom

The cone shaped phantom more closely resembles the characteristic shape of a pendant breast, with a tapering of the effective diameter of the phantom from the thick 'chest wall' to the 'nipple' area. As mentioned earlier, approximately 15% of pendant breasts from MRI scanned subjects have been characterized to have this geometry [32]. This dramatic tapering has an evident affect on the dose distributions, seen in the profiles in Figure 6.

There is a pronounced concavity in the water dose profile at the thickest section of the chest wall (profile #1 in Figure 6) with an approximate 50% difference between the peak periphery measured dose (~6mGy) and the center of the phantom (~4mGy). At this level the diameter of the cone is approximately 15cm wide, slightly wider than the cylindrical phantom altogether. The peak peripheral dose in the equivalent oil dose profile is more uniform with only approximately 17% greater dose at the edges than that of the central section of the phantom (~2.9mGy vs. 2.5mGy). In contrast to the cylindrical phantom, the dose profile for both the oil and water-filled conical phantom is more symmetrical about the vertical axis of rotation, likely due to more uniform centering of the phantom. Horizontal dose profiles progressively flatten closer to the nipple (see profile #2, Figure 6, generated at ~9cm diameter). The underlying reason for this is due to the decrease in effective phantom diameter. As the breast diameter decreases, the cumulative absorbed dose in the center of the breast, aggregated over the tomographic scan, increasingly approaches that of the entrance dose. Indeed, the convex appearance of Profile #3 in Figure 6, generated at a diameter of approximately 3.5cm, indicates that very close to the nipple, the center of the phantom cumulatively absorbs more dose than the skin.

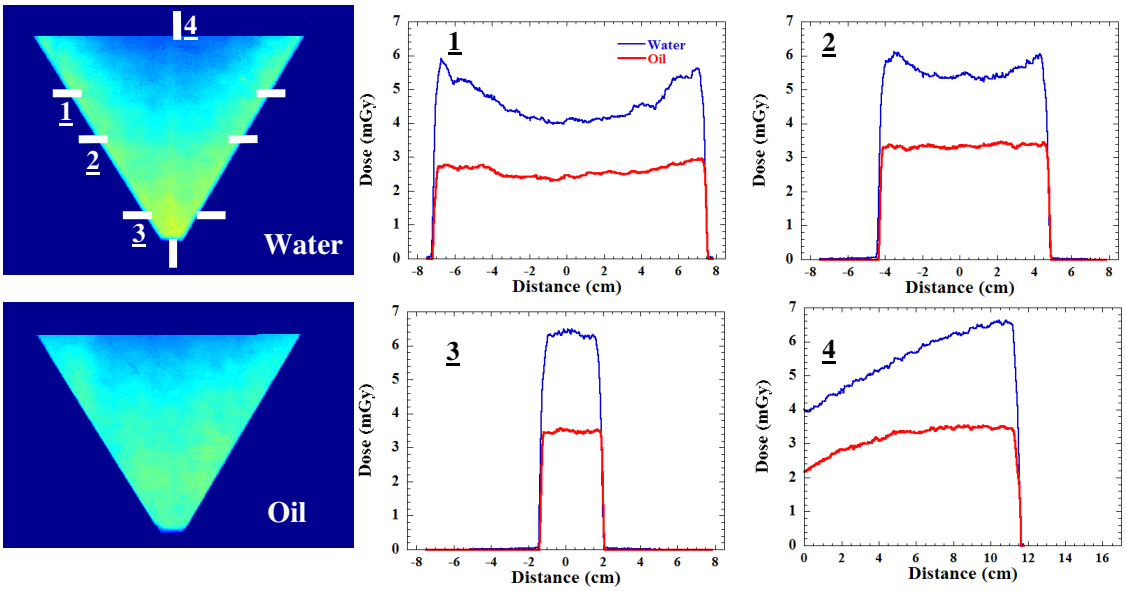

Figure 6 (Left) Color calibrated images of the absorbed dose in the water- and oil-filled conical phantom as measured by the radiochromic film, with (Right) accompanying horizontal and vertical profiles. Note the pronounced concave dose profile across the thickest section (profile #1, 'chest wall') of the cone, becoming less pronounced (profile #2) and turning convex as the effective diameter of the conical volume decreases near the nipple. (profile #3) Note also that the mean dose level increases closer to the nipple (profile #4). The >60% increase in dose between the chest wall and nipple is evidence of the influence that the breast diameter has on absorbed dose. The dose profile for water (equivalent 100% glandular tissue) is again consistently higher than that of the oil (equivalent 100% fatty tissue).

The increasing nature of Profile #4 in going from the chest wall towards the nipple further illustrates the increasing overall dose with decreasing phantom diameter. The skin (edge) dose remains relatively constant (~6mGy) as the breast diameter reduces, but the dose along the medial phantom increases from 4mGy at the chest wall to approximately 6.5mGy by the nipple region. The mean cumulative dose measured in the 2D conical cross section of the conical phantom is 5.3 ± 0.6mGy, and that of the oil phantom is 3.1 ± 0.3mGy.

A comparison plot of TLD "point dose" measurements in the conical water-filled phantom compared to dose measurements extracted from regions of interest (ROIs) on the co-registered radiochromic film image is shown in Figure 7. Only the 14 of the 19 TLD pair locations are reported that were immersed in the various fluids filling the phantom. The measured TLD values are averaged from four TLD measurements (2 TLD runs with pairs of TLDs located at each point, in each run). For comparison, the film measurements were generated using an ROI of the same size as the TLDs and were located at their corresponding positions in the image. TLD dose figures range from 2.5 - 5.2mGy with a mean dose of 3.7 ± 0.9mGy, and the equivalent figures for the radiochromic film are 3.8 ± 0.7mGy.

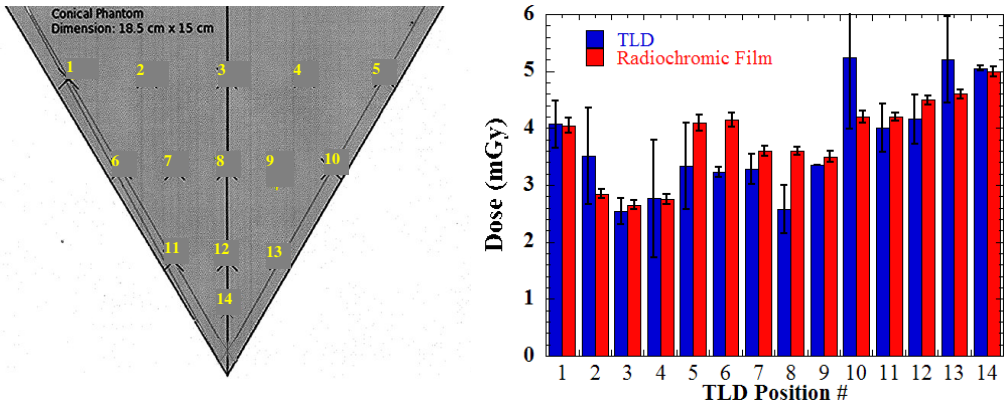

Figure 7 (Left) The conical template with the positions of the numbered TLD pairs. (Right) The average and standard deviation of the "point doses" measured from the TLDs in water compared to the dose at equivalent ROIs locations in the radiochromic film. Standard deviations for the radiochromic film was determined as the variation from the mean of the ROI in the film.

The figures for TLDs and radiochromic film therefore track each other very well, with most results within 10% of each other. The greatest discrepancies between the dosimeter measurements, however, are located towards the periphery of the triangular template. These differences can be attributed to slight inaccuracies during image registration, water seepage along the film edges, proximity to the water-air interface at that location, and differences in angular dependence (anisotropy) of response between the film and TLDs. While the calibration of the TLDs and the film was performed using a perpendicular exposure technique in air, the angular dependence of the responses was not explicitly characterized in this study. The overall close agreement between TLD and radiochromic film measurements serves to validate the film measurements that were evaluated throughout.

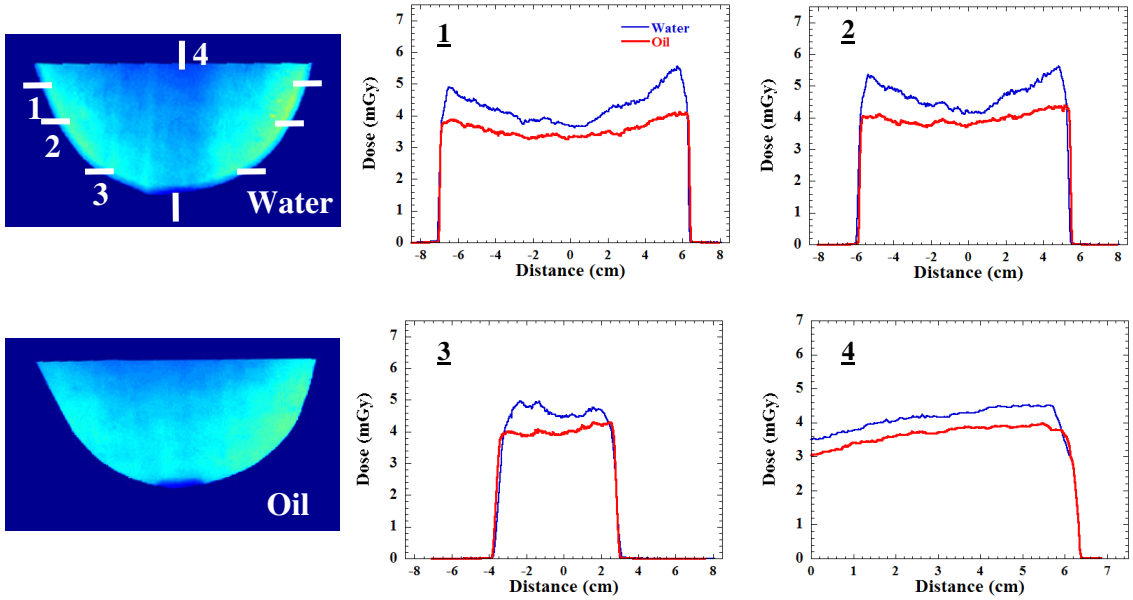

Figure 8 (Left) Color calibrated images of the absorbed dose in the water- and oil-filled anthropomorphic phantom measured by the radiochromic film with (right) accompanying horizontal and vertical profiles. Similar to the responses observed in the other phantoms, the horizontal dose profiles progressively flatten and the mean dose level increases approaching the nipple. The more rounded shape of the breast indicates that, unlike the conical phantom, the dose profile is not markedly convex at the nipple. The vertical dose profile indicates a 28% increase in dose along the center of the breast from the chest wall towards the nipple. The dose profile for water (equivalent 100% glandular tissue) is again consistently higher than that of the oil (equivalent 100% fatty tissue), but only nominally compared with the more geometric phantoms.

3.2.3. Anthropomorphic breast phantom

Figure 8 illustrates color calibrated images of the dose measured in the more clinically relevant anthropomorphic breast phantom, based on shape, size and density content. The mean dose measured in the water-filled phantom was 4.5 ± 0.4mGy and that of the oil-filled volume is 3.8 ± 0.2mGy. The results in Figure 8 also illustrate an increase in mean dose levels closer to the nipple, similar to the other geometric shapes. Evident in the profiles is the cupping close to the chest wall of the breast (profile #1 is generated at a breast diameter of 13.4cm) and the gradual flattening of the profile as the nipple is approached. However, the anthropomorphic breast does not taper near the nipple as sharply as the cone (the breast diameter for profile #3 is 7cm) and so the convex shaped profile that was present close to the nipple in the conical phantom is not present in the anthropomorphic breast phantom. Although not shown, overall measured dose levels for the sheet of radiochromic film placed orthogonally in the breast volume are identical to the one shown here. Furthermore, breast dose measured in oil is consistently higher than for the other geometric phantoms, and the reverse is true for the breast dose measured in water, making the point-wise differences between water and oil (glandular and adipose) smaller. All measurement procedures, radiochromic film immersion in the fluids, calibration and characterization procedures were identical to the earlier measurements. Thus, the greater similarity in the cumulative mean dose levels for both oil and water indicates that the breast geometry may play a larger role in overall absorbed dose than material content alone.

Histograms of dose figures (Figure 9, left) acquired across the 2D cross sections of both the oil- and water-filled anthropomorphic breast phantoms show a broader spectrum of dose values for the water-filled phantom. There is a slight skew towards the higher dose levels in water at the phantom's periphery, whereas dose in the oil filled phantom is more tightly distributed about the mean.

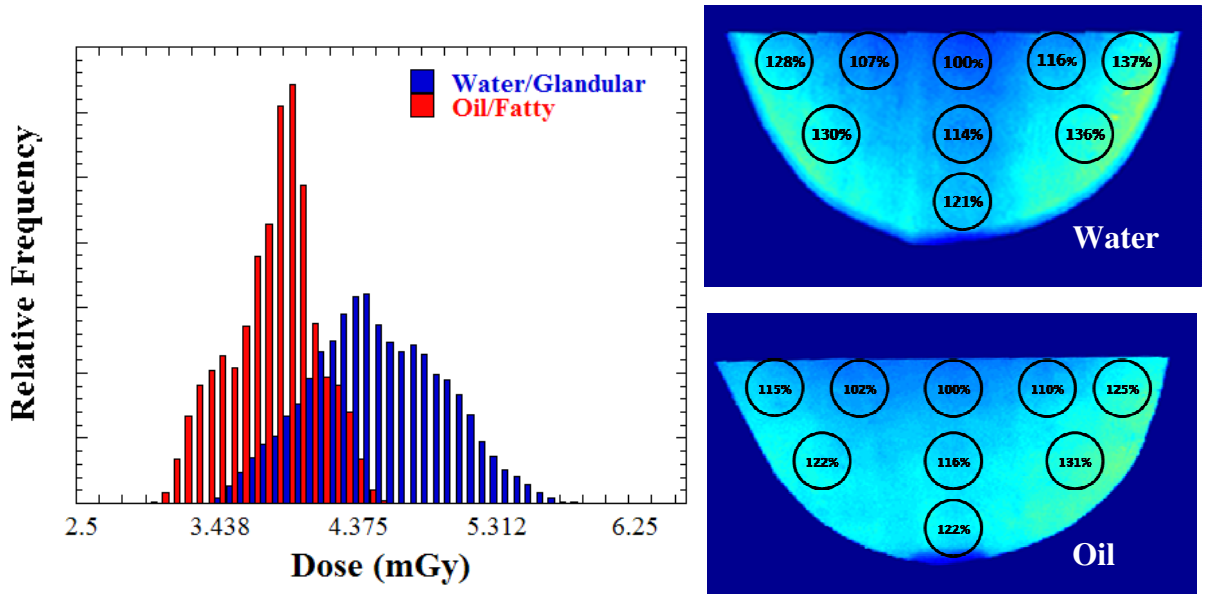

Figure 9 (Left) Histogram of dose measurements for the anthropomorphic breast volume filled with water (blue) and oil (red). The histograms illustrate the broader distribution of dose in the more glandular breast tissue compared to the fatty tissue. (Right) Percentage increase in dose normalized to the lowest dose in the center of the thickest part of the anthropomorphic breast for water (top) and oil (bottom).

A schematic plot of the variation in dose normalized to the center of the thickest section of the breast (Figure 9, right column) highlights the spatial trends seen in the profiles, where the periphery of the breast receives between 30-40% more dose than the central volume of the breast. Asymmetry is evident in the dose profile close to the chest wall of the breast phantom with the peak peripheral dose being between 20-30% greater than

the mean dose in the center of the phantom. This trend in increased periphery dose to the skin corroborates previous simulated and measured dosimetry experiments for breast CT[10, 13].

4. Conclusion

In this study, the doses deposited during tomographic scans of various geometric phantoms containing a wide range of simulated biological materials were measured using calibrated radiochromic film and TLDs fully immersed in the phantom volumes. The TLDs, a gold standard in dosimetry evaluation were used to cross-validate the radiochromic film. This measuring technique produced high resolution 2D dose distributions in geometric and breast shaped phantoms that can be extended to the 3D volume. Of particular interest was how the wide angle x-ray CT cone beam from the quasi-monochromatic source affected the dose distribution given various geometrical configurations, shapes and material contents of the 3D phantoms.

This dosimetry technique may be appropriately applied to a variety of breast imaging applications like planar mammography, tomosynthesis, and even nuclear emission imaging techniques in phantoms containing radiotracers (planar and 3D), as well as hybrid imaging applications.

The dose measured here was acquired on a single thin 2D plane, similar to a planar detector completely embedded inside the phantom of interest. If we invoke the symmetry in a couple the phantoms, then the resulting mean dose to the 3D breast from our dedicated breast CT system measured in anthropomorphic water- and oil-based phantoms appears to be comparable to those typical of dual view mammography, with average doses in oil (simulating 100% adipose tissue) of 3.8mGy and average dose in water (simulating 100% glandular) of 4.5mGy. Previous measurements calculated via Monte Carlo simulation[11-12, 17] are thus validated by these measurements.

The ACR upper limits for dual view mammography dose, 6mGy, were developed for a breast composition having a perceived 50-50% glandular-adipose tissue composition based on mammographic density measurements. The maximum absorbed dose figure in this study was generated using equivalent 100% glandular and 100% adipose tissue materials. The results in this study, combined with our previous observer study results, therefore suggest that the breast CT system and imaging protocol developed here may be able to tomographically image the uncompressed breast using less than the maximum allowable dose for dual view screening mammography. This imaging technique can certainly be used diagnostically, but also potentially in the screening domain where low cumulative radiation dose is a prerequisite.

Acknowledgments

This work was supported by NIH R01-CA096821, by DOD W81XWH-08-1-0352, by NIH/NIAID U19AI067798-01, and by the Department of Radiology, the Malek Foundation, the Duke Endowment and the James B. Duke Fellowship Program. MPT is the inventor of this hybrid breast imaging technology, and is named as an inventor on the patent for this technology assigned to Duke (US Pat. #7,609,808). If this technology becomes commercially successful, MPT and Duke could benefit financially.

References

1. S. J. Glick, "Breast CT," Annual Review of Biomedical Engineering **9**, 501-526 (2007).
2. R. L. McKinley, "Development and characterization of a dedicated computed mammotomography system," Ph. D.Thesis (2006).
3. L. Bassett, C. D'Orsi, C. Lee, P. Butler, R. Jong and B. Monsees, "Practice guidelines for the performance of screening and diagnostic mammography," (2008).
4. H. M. Warren-Forward and L. Duggan, "Towards in vivo TLD dosimetry in mammography," Br J Radiol **77**, 426-432 (2004).
5. X. Wu, G. T. Barnes and D. M. Tucker, "Spectral dependence of glandular tissue dose in screen-film mammography," Radiology **179**, 143-148 (1991).
6. D. R. Dance, "Monte-Carlo calculation of conversion factors for the estimation of mean glandular breast dose," Physics in Medicine and Biology **35**, 1211 (1990).
7. D. R. Dance, A. Thilander-Klang, M. Sandborg, C. L. Skinner, A. Castellano-Smith and G. Alm-Carlsson, "Influence of anode/filter material and tube potential on contrast, signal-to-noise ratio and average absorbed dose in mammography: a Monte Carlo study," Brit. J. Radiol. **73**, 1056-1067 (2000).
8. D. R. Dance, R. A. Hunt, P. R. Bakic, A. D. A. Maidment, M. Sandborg, G. Ullman and G. Alm Carlsson, "Breast dosimetry using high-resolution voxel phantoms," Radiat Prot Dosimetry **114**, 359-363 (2005).
9. J. M. Boone, N. Shah and T. R. Nelson, "A comprehensive analysis of DgN_{CT} coefficients for pendant-geometry cone-beam breast computed tomography," Medical Physics **31**, 226-235 (2004).
10. S. C. Thacker and S. J. Glick, "Normalized glandular dose (DgN) coefficients for flat-panel CT breast imaging," Physics in Medicine and Biology **49**, 5433 (2004).
11. J. M. Boone, T. R. Nelson, K. K. Lindfors and J. A. Siebert, "Dedicated breast CT: radiation dose and image quality evaluation," Radiology **221**, 657-667 (2001).
12. B. Chen and R. Ning, "Cone-beam volume CT mammographic imaging: feasibility study," Med. Phys. **29**, 755-770 (2002).
13. P. Russo, A. Lauria, G. Mettivier and M. C. Montesi, presented at the Nuclear Science Symposium Conference Record, 2008 (unpublished).
14. P. Russo, T. Coppola, G. Mettivier, M. C. Montesi and A. Lauria, presented at the IEEE Nuclear Science Symosium and Medical Imaging, Orlando, Florida, 2009 (unpublished).
15. P. Madhav, S. J. Cutler, D. C. Crotty, K. L. Perez, R. L. McKinley, L. Wilke, T. Wong and M. P. Tornai, "Pilot Patient Studies Using a Dedicated Dual-Modality SPECT-CT System for Breast Imaging " in *2008 AAPM,* (Houston TX, 2008).
16. M. P. Tornai, R. L. McKinley, C. N. Brzymialkiewicz, P. Madhav, S. J. Cutler, D. J. Crotty, J. E. Bowsher, E. Samei and C. E. Floyd, "Design and development of a fully-3D dedicated x-ray computed mammotomography system," Proc SPIE: Phys Med Imag **5745**, 189-197 (2005).
17. R. L. McKinley and M. P. Tornai, "Preliminary investigation of dose for a dedicated mammotomography system," Proc SPIE: Phys Med Imag **6142**, 60-70 (2006).
18. M. J. Yaffe, J. M. Boone, N. Packard, O. Alonzo-Proulx, S. Y. Huang, C. L. Peressotti, A. Al-Mayah and K. Brock, "The myth of the 50-50 breast," Medical Physics **36**, 5437-5443 (2009).
19. R. L. McKinley, M. P. Tornai, E. Samei and M. L. Bradshaw, "Simulation study of a quasi-monochromatic beam for x-ray computed mammotomography," Med. Phys. **31**, 800-813 (2004).
20. D. J. Crotty, R. L. McKinley and M. P. Tornai, "Experimental spectral measurements of heavy K-edge filtered beams for x-ray computed mammotomography," Physics in Medicine and Biology **52**, 603-616 (2007).

21. R. L. McKinley, M. P. Tornai, E. Samei and M. L. Bradshaw, "Development of an optimal x-ray beam for dual-mode emission and transmission mammotomography," Nucl. Instr. Meth. Phys. Res. A **527**, 102-109 (2003).
22. A. Rink, I. A. Vitkin and D. A. Jaffray, "Characterization and real-time optical measurements of the ionizing radiation dose response for a new radiochromic medium," Medical Physics **32**, 2510-2516 (2005).
23. S. Devic, N. Tomic, Z. Pang, J. Seuntjens, E. B. Podgorsak and C. G. Soares, "Absorption spectroscopy of EBT model GAFCHROMIC[sup [trademark sign]] film," Medical Physics **34**, 112-118 (2007).
24. H. Alva and et al., "The use of a reflective scanner to study radiochromic film response," Physics in Medicine and Biology **47**, 2925 (2002).
25. G. Thomas, R. Y. L. Chu and F. Rabe, "A study of GafChromic XR type R film response with reflective-type densitometers and economical flatbed scanners," Journal of applied clinical medical physics **4**, 307-314 (2003).
26. B. C. Ferreira and et al., "Evaluation of an Epson flatbed scanner to read Gafchromic EBT films for radiation dosimetry," Physics in Medicine and Biology **54**, 1073 (2009).
27. L. Paelinck, W. De Neve and C. De Wagter, "Precautions and strategies in using a commercial flatbed scanner for radiochromic film dosimetry," Phys Med Biol **52**, 231-242 (2007).
28. S. Devic, N. Tomic, C. G. Soares and E. B. Podgorsak, "Optimizing the dynamic range extension of a radiochromic film dosimetry system," Med Phys **36**, 429-437 (2009).
29. A. Niroomand-Rad, C. R. Blackwell, B. M. Coursey, K. P. Gall, J. M. Galvin, W. L. McLaughlin, A. S. Meigooni, R. Nath, J. E. Rodgers and C. G. Soares, "Radiochromic film dosimetry: recommendations of AAPM Radiation Therapy Committee Task Group 55. American Association of Physicists in Medicine," Med Phys **25**, 2093-2115 (1998).
30. S. Devic, J. Seuntjens, E. Sham, E. B. Podgorsak, C. R. Schmidtlein, A. S. Kirov and C. G. Soares, "Precise radiochromic film dosimetry using a flat-bed document scanner," Med Phys **32**, 2245-2253 (2005).
31. Y. S. Horwitz, *Thermoluminescence and Thermoluminescent Dosimetry*. (CRC Press, 1984).
32. S. J. Cutler, D. J. Crotty and M. P. Tornai, presented at the Nuclear Science Symposium Conference Record, 2008. NSS '08. IEEE, 2008 (unpublished).
33. A. L. C. Kwan, J. M. Boone and N. Shah, "Evaluation of x-ray scatter properties in a dedicated cone-beam breast CT scanner," Medical Physics **32**, 2967-2975 (2005).

APPENDIX D: Doctoral Thesis Abstract

This thesis research builds upon prior work that developed separate SPECT and CmT (computed mammotomography, or breast CT) devices that were independently capable of imaging an uncompressed breast in 3D space. To further develop the system as a clinically viable device, it was necessary to integrate the separate imaging systems onto a single gantry, and to then design a patient-friendly bed that could routinely and effectively position the patient during dual modality imaging of her uncompressed breast in the system's common field of view. This thesis describes this process and also investigates practical challenges associated with dedicated breast imaging of a prone patient using the integrated SPECT-CT device.

We initially characterized the practicability of implementing the novel x-ray beam ultra-thick K-edge filtration scheme designed for routine use with the breast CT system. Extensive computer simulations and physical measurements were performed to characterize the x-ray beam produced using K-edge filtration with cerium and to compare it to beams produced using other filtration methods and materials. The advantages of using this heavily filtered x-ray beam for uncompressed breast CT imaging were then further evaluated by measuring the dose absorbed by an uncompressed cadaver breast during the course of a routine tomographic scan. It was found that the breast CT device is indeed capable of imaging uncompressed breasts at dose levels below that of the maximum allowed for dual view screening mammography.

To prepare the separate SPECT and CT systems for integration onto a single platform, the cross contamination of the image of one modality by primary and scattered photons of the other modality was quantified. The separate SPECT and CT systems were then integrated, and a patient friendly bed was designed for the newly integrated system using a combination of computer aided design and lab-based testing methods. The performance of the system was evaluated during early stage dual modality patient imaging trials with particular emphasis placed on the performance of the patient bed. The bed was successful in its primary task of enabling dual modality imaging of a patients' breast in the common field of view, but practical challenges to more effective patient imaging were identified as well as some novel solutions to these challenges.

In the final section of the thesis research, the feasibility of using two of these solutions were investigated with a view to imaging more of the patients' posterior breast volume. Limited angle tomographic trajectories and trajectories that involve raising or lowering the patient bed in mid tomographic acquisition were initially investigated using various geometric phantoms. A very low contrast imaging task was then tested using an observer study to quantify the effect of these trajectories on the ability of observers to maintain visibility of small geometric objects.

This initial integrated SPECT-CT imaging system has demonstrated its ability to successfully perform low dose, dual modality imaging of the uncompressed breast. Challenges and solutions have been identified here that will make future SPECT-CT designs even more powerful and clinically relevant technique for molecular imaging of the breast.